

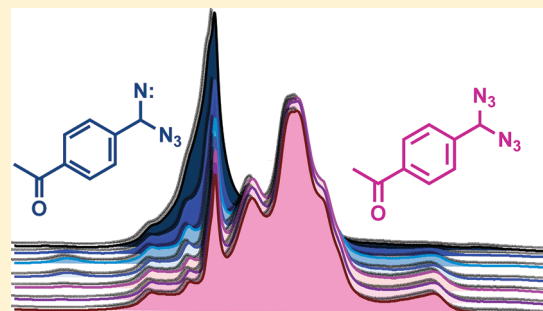
Triplet-Sensitized Photoreactivity of a Geminal Diazidoalkane

Ranaweera A. A. Upul Ranaweera, Jagadis Sankaranarayanan, Lydia Casey, Bruce S. Ault, and Anna D. Gudmundsdottir*

Department of Chemistry, University of Cincinnati, Cincinnati, Ohio 45221-0172, United States

S Supporting Information

ABSTRACT: Photolysis of **1** in chloroform yielded **2** as the major product and a small quantity of **3**. Laser flash photolysis demonstrated that upon irradiation, the first excited triplet state of the ketone (T_{1K}) of **1** is formed and decayed to form radical **4**, which has a λ_{\max} at 380 nm ($\tau = 2 \mu\text{s}$). Radical **4** expelled a nitrogen molecule to yield imine radical **5** (λ_{\max} at 300 nm). Density functional theory (DFT) calculations showed that the transition state barrier for the formation of **5** is approximately 4 kcal/mol. In comparison, photolysis of **1** in argon matrices resulted in triplet nitrene **6**, which was further characterized with ^{15}N and D isotope labeling and DFT calculations. Prolonged irradiation of **6** yields triplet imine nitrene **7**.

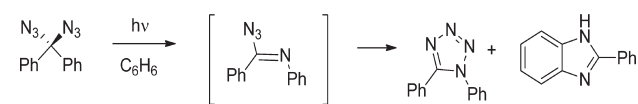


1. INTRODUCTION

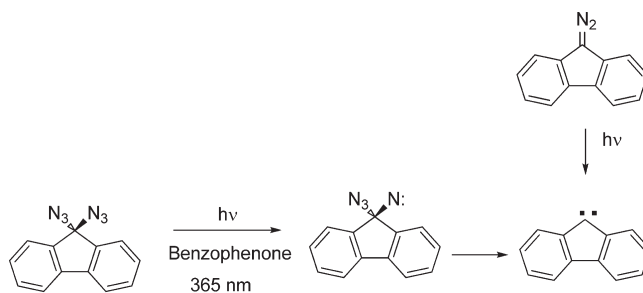
Excitation of aryl azides causes them to fall apart, expel a nitrogen molecule, and form singlet aryl nitrenes.¹ At a cryogenic temperature, the singlet aryl nitrene intersystem crosses to its triplet configuration. Photolysis of aryl azides at low temperatures has been used to successfully form triplet aryl nitrenes and high-spin quintet aryl dinitrenes and septet aryl trinitrenes from the corresponding diaryl and triaryl azides.^{2–6} In comparison, triplet alkyl nitrenes cannot be formed by direct irradiation of alkyl azides because they yield imine products. Kyba and Abramovitch theorized that the singlet excited state of the alkyl azides reacted in a concerted manner to form the imine products.⁷ However, they also hypothesized that photolysis of the alkyl azides resulted in singlet alkyl nitrenes that rearrange to form the imine products faster than they undergo intersystem crossing to the triplet state.⁸ In comparison, triplet-sensitized photolysis of alkyl azides has been shown to be efficient in forming triplet alkyl nitrenes, both at ambient and cryogenic temperatures.^{9–13}

The photochemistry of diazido alkanes has not been studied extensively; however, Moriarty and Kliegman have shown that direct irradiation of diazidodiphenylmethane results in the formation of 1,5-diphenyltetrazole and a small amount of 2-phenylbenzimidazole (Scheme 1). This reaction presumably occurs by singlet reactivity of the excited state of the azido chromophore to form an imine that reacts further.^{14,15} In addition, Barash et al. have shown that photolysis of 9,9-diazido-9H-fluorene with benzophenone as a triplet sensitizer yielded an ESR signal that can be attributed to the formation of the corresponding mononitrene (Scheme 2).¹⁶ Prolonged irradiation at 365 nm led to the formation of the triplet carbene shown in Scheme 2. The formation of the triplet carbene intermediate was verified by irradiation of the diazo precursor, which also yielded the same ESR signal.

Scheme 1



Scheme 2

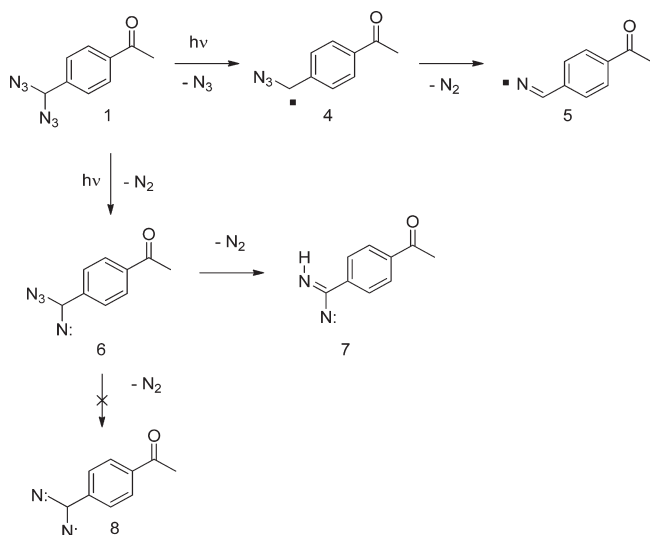


In this paper, we describe the triplet reactivity of diazido derivative **1**. Product studies, laser flash photolysis, phosphorescence, matrix isolation, isotope labeling, and density functional theory (DFT) calculations were used to elucidate the reactivity of **1**. Photolysis of **1** in solution yielded primarily **2** by homolytic cleavage of one of the azido groups. In argon matrices, triplet nitrene **6** was the major product. Prolonged irradiation of **6** yielded triplet imine nitrene **7** rather than quintet dinitrene **8** in argon matrices (Scheme 3).

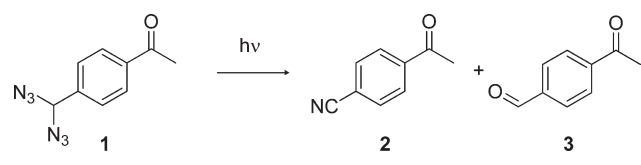
Received: June 21, 2011

Published: September 06, 2011

Scheme 3



Scheme 4



2. RESULTS

2.1. Product Studies. Photolysis of **1** in argon-saturated chloroform-*d* through a Pyrex filter at 196 K yielded **2** as the major product, along with a small amount of **3** (Scheme 4). Irradiation of **1** through a Pyrex filter ensured that only the ketone chromophore absorbed the light and formed the singlet excited state of the ketone (S_{1K}), as alkyl azides only have a weak absorption below approximately 300 nm.^{10,17,18} Because **1** is an acetophenone derivative, the S_{1K} of **1** is expected to intersystem cross to its triplet excited state, and the first and the second excited states of the triplet ketone (T_{1K} and T_{2K}) are within a few kcal/mol of each other.^{18–20} Energy transfer from T_{1K} or T_{2K} of **1** to the azido moiety formed the triplet excited state of the azide chromophore (T_A) in **1**, which can fall apart to yield triplet nitrene **6** and a nitrogen molecule (Scheme 5). Several other intramolecular sensitizations of alkyl azides have been reported from triplet alkyl nitrenes.^{9,12} Because products **2** and **3** have less than two nitrogen atoms, it is not likely that **6** reacts further to form dinitrene **8**. Instead, the C– N_3 bond in **6** cleaves to form **5** and an azido radical. It can also be theorized that a radical abstracts a hydrogen atom from **6** to form **9**. Radical **9** can cleave to form **2**, whereas **5** can result in both **2** and **3**, as shown in Scheme 5.

It is also possible that photolysis of **1** does not form triplet nitrene **6**, but the azido group cleaves to yield an azido radical and **4**, which rearranges to form **5** (Scheme 6). We have previously reported that intramolecular sensitization of alkyl azides can result in cleavage of azido groups^{21,22} and that a radical adjacent to an azido group rearranges to form imine radicals.²³

We photolyzed **1** in argon-saturated toluene to verify whether any new products were observed in solvent with abstractable H atoms. GC–MS analysis of the reaction mixture showed the formation of **2** and **3** as the major products, in addition to **10**, which can be attributed to trapping imine radical **5** with a benzyl radical (Scheme 7). Furthermore, 1,2-diphenylethane was detected and must have been derived from the solvent by dimerization of two benzyl radicals. A small amount of **11** was also formed in toluene. In oxygen-saturated toluene, the major products were **2** and small amounts of **3** and **11**. Product studies in toluene support that irradiation of **1** results in radical **5**, and in an oxygen-saturated solution, oxygen reacts with radical **5** to form **2**. Furthermore, we theorized whether **3** and **11** can be attributed to the formation of a triplet carbene intermediate.

2.2. Phosphorescence. The phosphorescence of **1** was measured in ethanol glasses at 77 K (Figure 1). The (0,0) band for the phosphorescence was estimated to be approximately 407 nm; thus, the energy of the first excited triplet ketone (T_{1K}) of **1** was calculated to be 70 kcal/mol, which is approximately 2 and 3 kcal/mol lower than observed for the analogous *p*-methyl acetophenone and *p*-trifluoromethyl acetophenone.²⁴

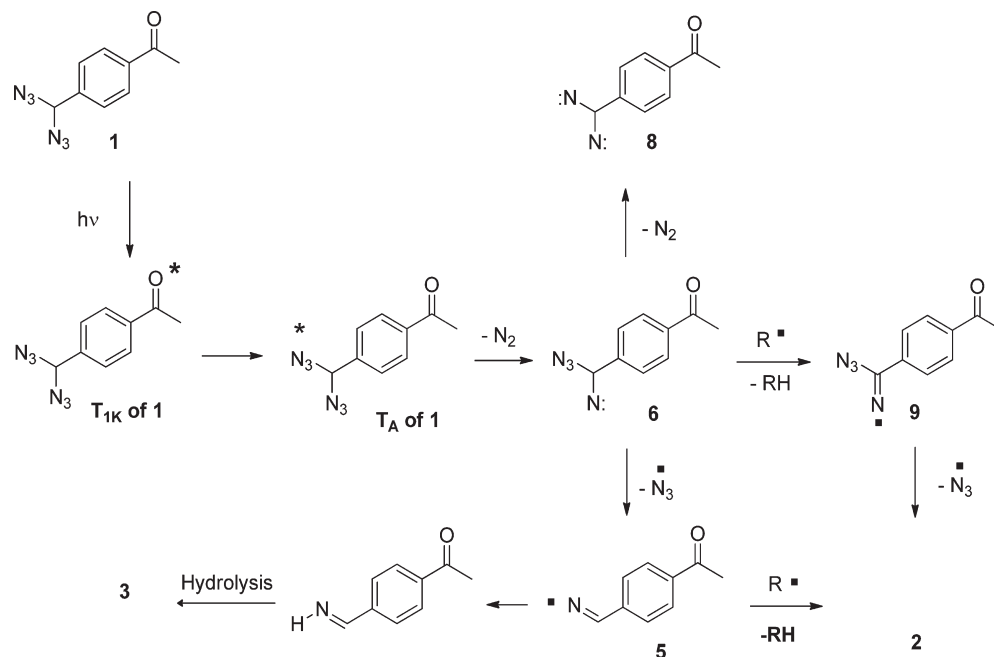
2.3. Calculations. The stationary points on the triplet and quintet surface of **1** were calculated to better understand the factors governing the reactivity of **1** using Gaussian09²⁵ at the B3LYP level of theory with the 6-31+G(d) basis set.^{26,27}

The ground-state (S_0) of **1** was optimized in the gas phase, and several minimal energy conformers were found (see Supporting Information) due to the azido groups. The conformer of **1** was used for the calculations in which the azido groups are lined up, as shown in Figure 2. This conformer was selected for the calculations because its calculated IR spectrum contained an azido stretch at 2257 cm^{-1} ($f = 109$) and 2250 ($f = 995$) due to symmetrical and antisymmetrical stretching of the two azido groups, respectively (f is the calculated oscillator strength). The neat IR spectrum of **1** had a strong azido band at 2105 cm^{-1} . The other low energy conformers of **1** contained two azido bands with similar oscillator strengths, but their frequencies were better resolved. The S_0 geometry of **1** was used to perform TD-DFT calculations,^{28–32} which located the first excited triplet ketone (T_{1K}) of **1** at 72 kcal/mol above the ground state (S_0) in the gas phase (Scheme 8). Inspection of the molecular orbitals shows that T_{1K} of **1** has a (n, π^*) configuration, whereas T_{2K} is 76 kcal/mol above S_0 and has a (π, π^*) configuration. Thus, the TD-DFT calculations yielded a vertical excitation energy for T_{1K} of **1**, which is similar to the result obtained from the phosphorescence of **1**.

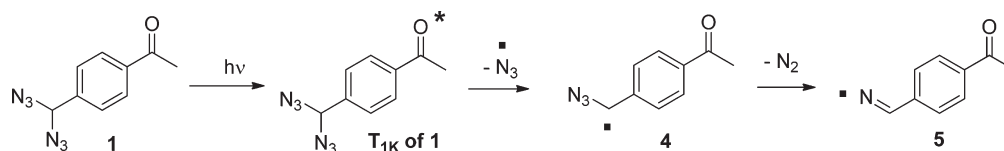
Optimization of the T_{1K} of **1** found that it is located 67 kcal/mol above S_0 , which is considerably lower energy than the numbers obtained by TD-DFT calculations and the phosphorescence spectrum. Inspection of the molecular orbitals and the C=O bond in T_{1K} , elongated to 1.321 Å, indicated that the optimized structure of T_{1K} of **1** had a (n, π^*) configuration. The bond lengths and bond angles of the azido moiety in T_{1K} of **1** were similar to the corresponding bonds and angles in the S_0 of **1**, demonstrating that the T_{1K} of **1** was localized on the acetophenone moiety. It should be noted that we have previously shown that density functional calculations underestimate the energy of triplet ketones with (n, π^*) configurations.^{18,22,33}

The triplet excited state of the azido group (T_A) in **1** that is located 44 kcal/mol above the S_0 was also optimized. The N–N–N bond in the T_A of **1** has a bond angle of approximately 120.4° and a N1–N2 bond length of 1.423 Å. Additionally, the

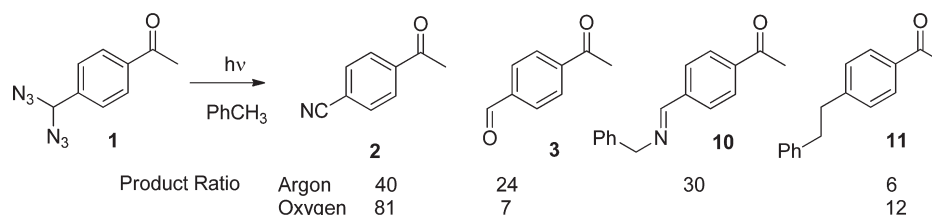
Scheme 5



Scheme 6



Scheme 7



bond length and the bond angle of the carbonyl group is similar to the corresponding bond length and bond angle in the S_0 of **1**, indicating that this triplet excited state is localized on the azido moiety. The triplet transition state for the T_A of **1** to cleave and form **6** (T_N) and a N_2 molecule is located only 0.1 kcal/mol above the T_A of **1**. Thus, the energy of T_A in **1** and the transition state for forming a nitrene is similar to what was reported for monosubstituted alkyl azides.^{18,22} The triplet transition state was located for **6** forming **7** (T_{im}) by simultaneously expelling a nitrogen molecule and undergoing a 1,2-H atom shift 40 kcal/mol above **6**, which was similar to what Nguyen et al. have reported for azidomethane.³⁴

The triplet transition state for **1** to cleave and form an azido radical and **4** was calculated. It was determined that it was located

approximately 3 kcal/mol below the T_{IK} of **1** (Scheme 9). Intrinsic reaction coordinate (IRC) calculations^{35,36} correlated this transition state with **4** and the azido radical and a triplet excited state that has an elongated C–N bond. However, UB3LYP calculations cannot be used to optimize the triplet excited state because it is not the lowest triplet excited state of the azido or aryl ketone chromophores.

Additionally, we calculated the quintet excited state of the azido chromophore (T_A) of **6** and found that it was located 46 kcal/mol above the ground state of **6**, and the transition state for the T_A of **6** to form **8** was located 0.1 kcal/mol above the T_A of **6** (Scheme 10). The energy surface for **6** to form **8** was similar to what was observed for the T_A of **1** to form **6**. However, **8** was destabilized by 2 kcal/mol in comparison to **6**.

Finally, the quintet transition state for **8** undergoing 1,2-H atom shift to form quintet nitrene **7** (Scheme 10) was calculated and located 48 kcal/mol above **8**. The calculations indicated that quintet imine-nitrene **7** was 9 kcal/mol more stable than quintet dinitrene **8**. Triplet imine nitrene **7** was 61 kcal/mol more stable than **6** due to the release of the N_2 molecule and because the nitrene moiety was stabilized *via* conjugation with the imine chromophore.

The triplet transition state for **6** cleaving to form **5** and an azido radical was located 9 kcal/mol above **6** (Scheme 11). Similarly, the transition state for radical **9** to cleave to form an

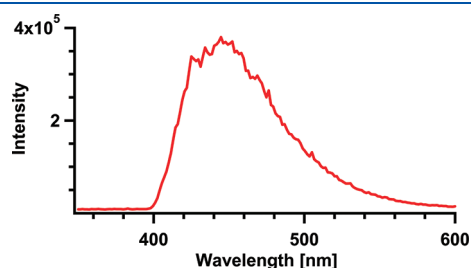


Figure 1. Phosphorescence spectrum of **1** in ethanol at 77 K, as obtained by 300 nm irradiation.

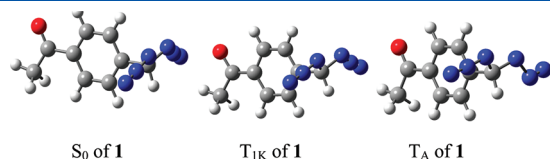


Figure 2. Optimized structure of **1**, T_{1K} of **1**, and T_A of **1**.

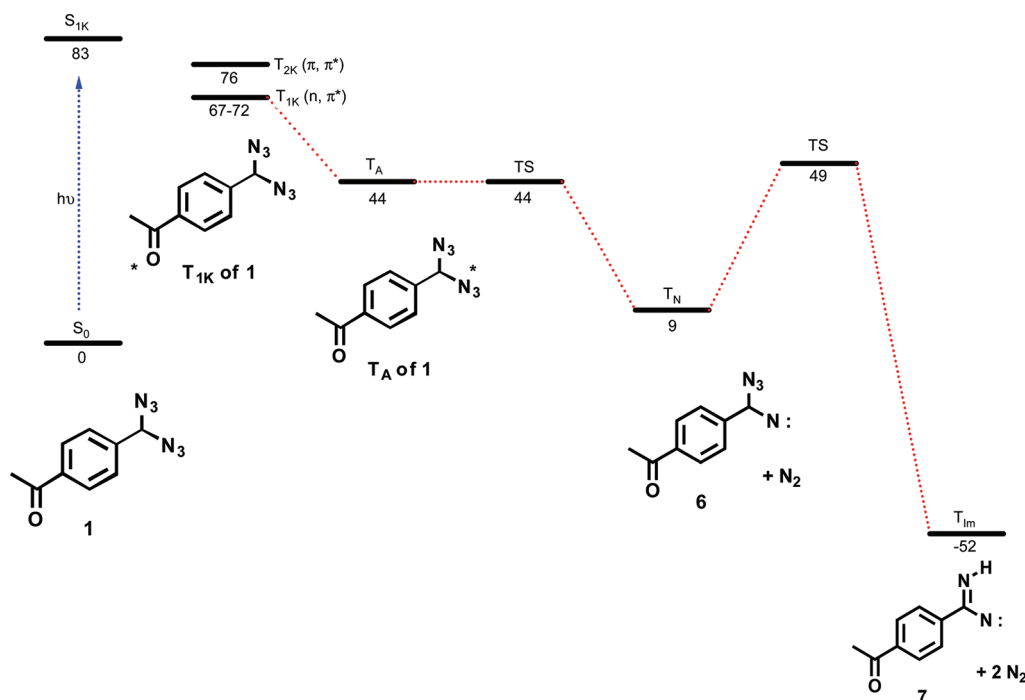
azido radical and **2** was located 11 kcal/mol above **9**. The calculations supported that **6** and **9** can be expected to undergo azido cleavage at ambient temperature. Finally, the transition state for **5** abstracting a H atom from toluene was calculated and located 15 kcal/mol above **5**. Therefore **5** is anticipated to be a long-lived intermediate because it is not expected to abstract H atoms from the solvent efficiently, but rather toluene or azido radicals are more likely to abstract a H atom from **5**.

The optimized structures of nitrenes **6**, **7**, and **8** (Scheme 12) were compared. In **6**, the C–N bond for the nitrene moiety was 1.425 Å, whereas in **8**, the C–N bonds increased to 1.440 Å due to the electronic repulsions between the two nitrene units (Scheme 12). Furthermore, the electron repulsion caused the N–C–N bond angle to increase to 114.1° in **8** from 109.1° in **6**. In comparison, the C–N bond in **7** was shorter because the nitrene and imine moieties were conjugated. The calculations show that the spin density was localized on the nitrogen atoms in **6** and **8**, whereas in **7**, the conjugation delocalized the spin density over the N-nitrene and iminyl moieties.

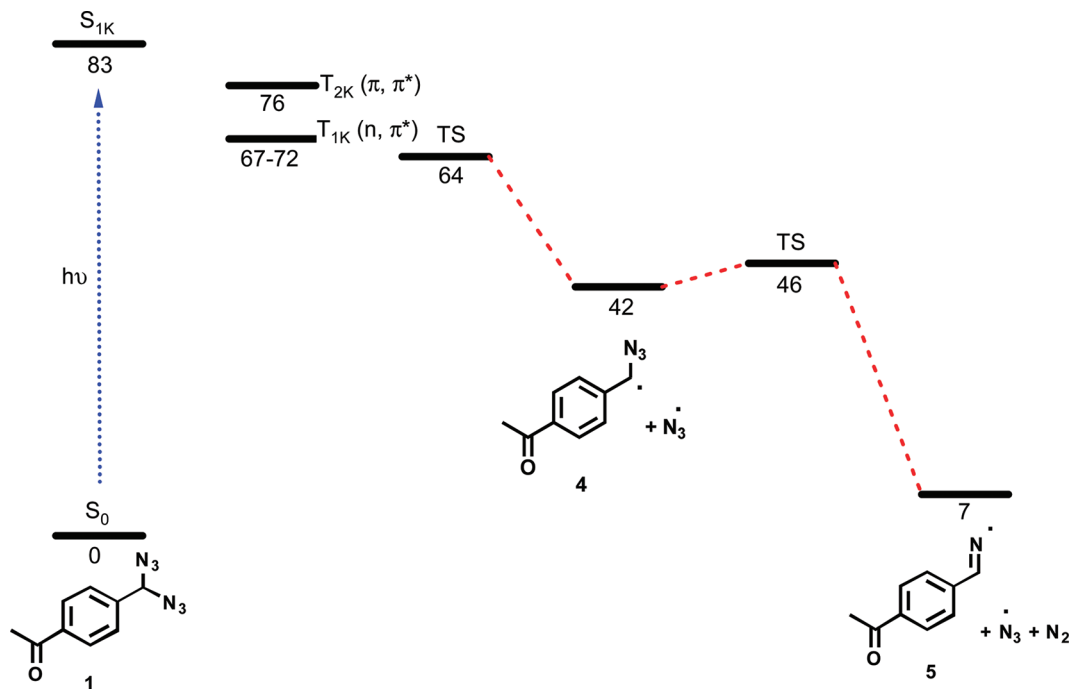
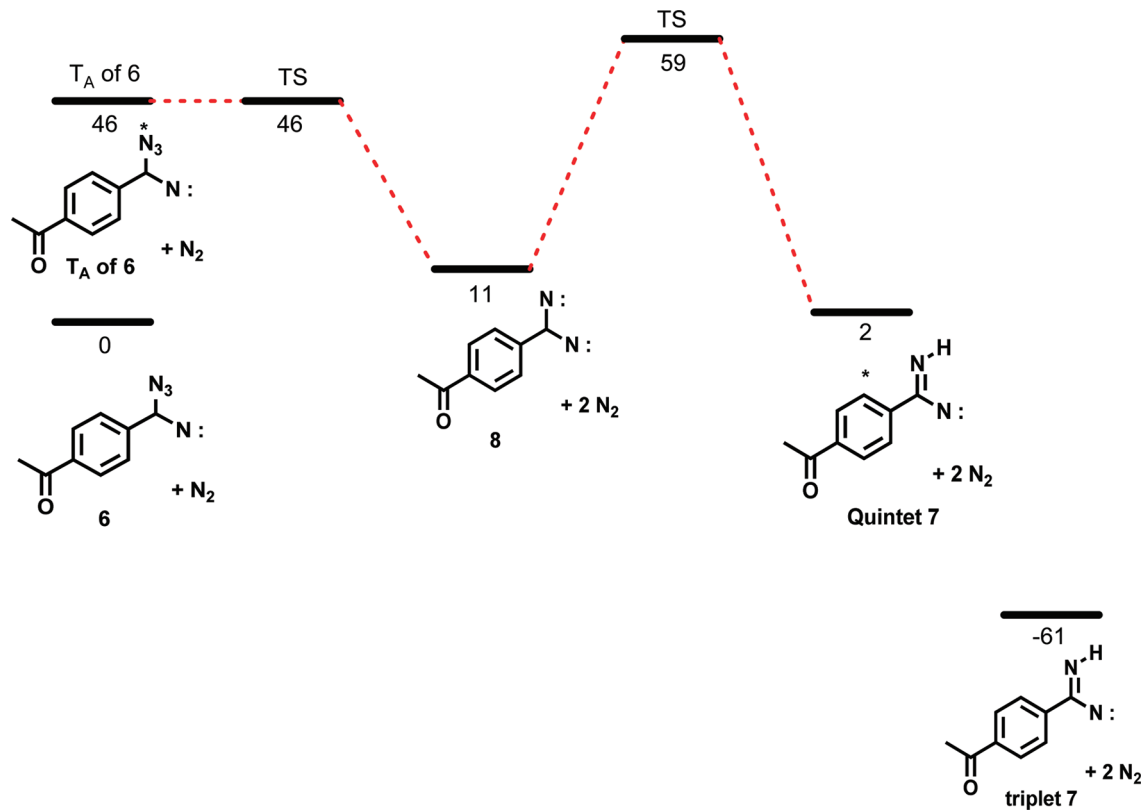
The calculations indicated that on the triplet surface, **1** can easily both undergo azido cleavage to form radical **4** (Scheme 9) and energy transfer to form triplet alkyl nitrene **6** (Scheme 8). However, it is not likely that quintet dinitrene **8** is formed from photolysis of **6**, but rather the more stable triplet iminyl nitrene **7** (Scheme 10).

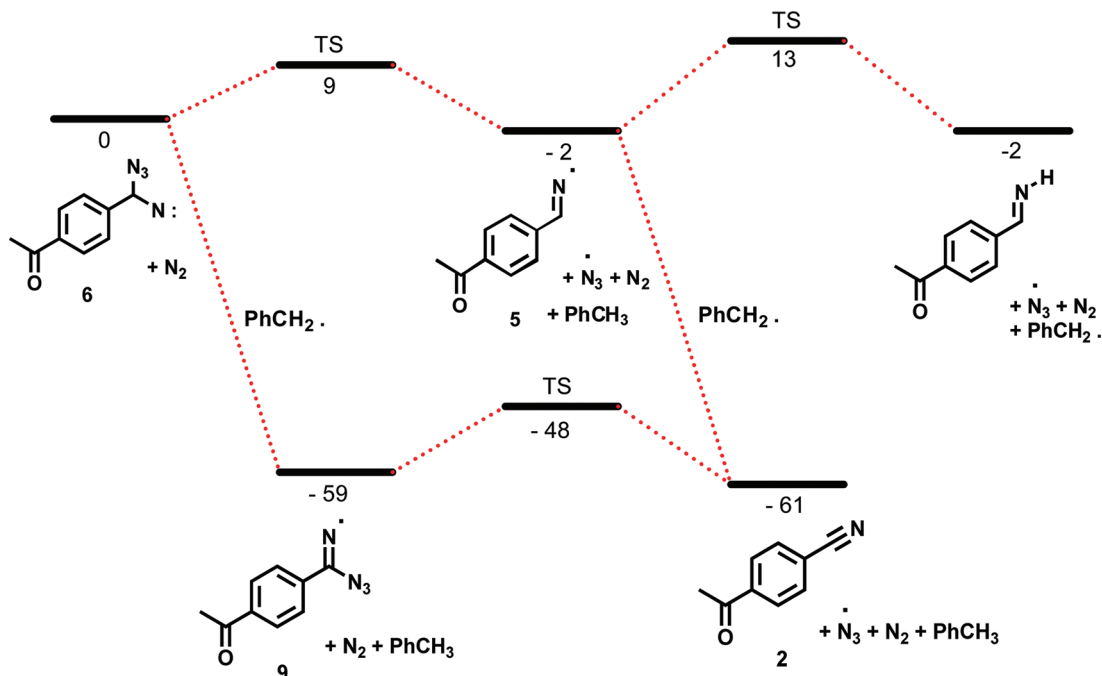
2.4. Laser Flash Photolysis. Laser flash photolysis of **1** was performed to elucidate the triplet reactivity of **1** at ambient temperature in solution. Laser flash photolysis (Excimer laser, $\lambda = 308$ nm, 17 ns)²³ of **1** in argon-saturated acetonitrile produced transient absorptions with λ_{max} at approximately 400 and 480 nm (Figure 3). As the intensity of these bands decreased with time, a new absorption with a λ_{max} at 330 nm was formed (Figure 3). The calculated (TD-DFT) absorption

Scheme 8. Calculated (B3LYP/6-31+G(d)) Stationary Points on the Triplet Surface of **1** To Form Nitrene **6** and **7**^a



^a Energies are in kcal/mol.

Scheme 9. Calculated (B3LYP/6-31+G(d)) Stationary Points on the Triplet Surface of 1 for Azido Cleavage^a^a Energies are in kcal/mol.Scheme 10. Calculated (B3LYP/6-31+G(d)) Stationary Points on the Triplet and Quintet Surfaces of 6 Forming 8 and 7^a^a Energies are in kcal/mol.

Scheme 11. Calculated (B3LYP/6-31+G(d)) Stationary Points on the Triplet Surfaces of **6** for Formation of **4** and **5**^a^aEnergies are in kcal/mol.Scheme 12. C–N Bond Lengths and N–C–N Bond Angles in **1**, **6**, **7**, and **8**

N-C-N Angle:	102.6°	109.1°	114.1°	117.6°
	1	6	8	7
C-N ₃ bond length (Å)	1.479	1.507	1.440	1.327
C-N bond length (Å)		1.425		

spectrum of T_{1K} of **1** contained major electron transitions at 461 ($f = 0.027$), 438 ($f = 0.0087$), 376 ($f = 0.0127$), 313 ($f = 0.0276$), and 300 nm ($f = 0.0372$), where f is the calculated oscillator strength (Figure 4). In addition, the calculated absorption spectrum of **4** in acetonitrile had a major electronic transition at 500 ($f = 0.1115$), 362 ($f = 0.3084$) and 353 nm ($f = 0.4529$), as shown in Figure 4. The transient spectrum obtained at shorter time scales was assigned to T_{1K} of **1** and **4**. In comparison, the calculated spectrum for **5** contained major electronic transitions at 286 ($f = 0.0378$) and 271 nm ($f = 0.551$) and a smaller one at 345 nm ($f = 0.0004$). Because of the intense band at 271 nm we propose that the absorption for **5** trails out to 330 nm, which fits with the transient spectrum obtained at a longer time scale (Figure 3). It should be highlighted that there is some residual absorption at 330 nm due to product formation in addition to absorption of **5**.

In oxygen-saturated acetonitrile, the transient absorption was reduced and the λ_{max} shifted to 380 nm, which was assigned to **4** (Figure 3).

Kinetic analysis of the transient absorptions in acetonitrile further supported these assignments. In argon-saturated acetonitrile, the transient absorption due to **4** (480 nm) was formed at a rate constant of $1.0 \times 10^7 \text{ s}^{-1}$ and decayed with a rate constant of $5 \times 10^5 \text{ s}^{-1}$ (Figure 5a). Because the absorption coefficient for T_{1K} of **1** was less at 480 nm than for **4**, the growth of **4** was observed rather than the decay of T_{1K} of **1**. The rate for forming **5** was measured at 340 nm and was the same within experimental error as the decay for **4** (Figure 5b). Radical **5** was long-lived with a decomposition rate constant of $4 \times 10^2 \text{ s}^{-1}$ (Figure 6a).

In addition, a small amount of growth, with a rate constant of $3.3 \times 10^3 \text{ s}^{-1}$, was observed at 340 nm (Figure 6b). We theorized that this transient was due to radical **5** being formed from triplet

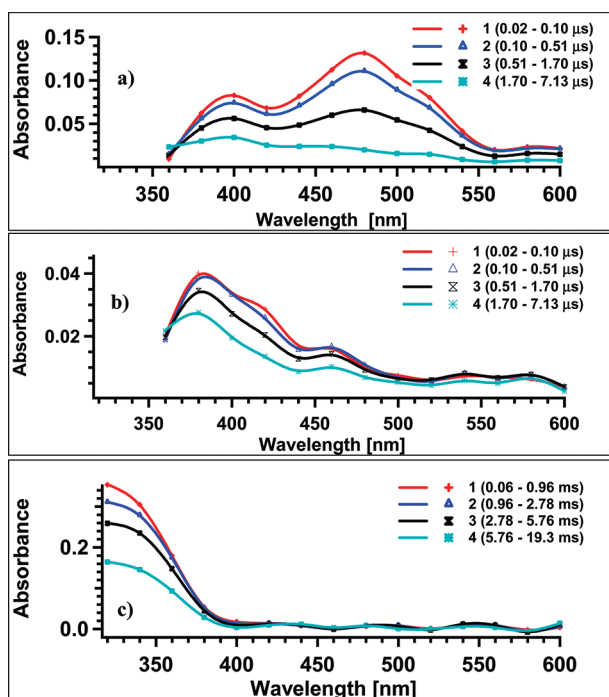


Figure 3. Laser flash of **1** (a) in argon-saturated acetonitrile at a short time scale, (b) in oxygen-saturated acetonitrile at a short time scale, and (c) in argon-saturated acetonitrile at a longer time scale.

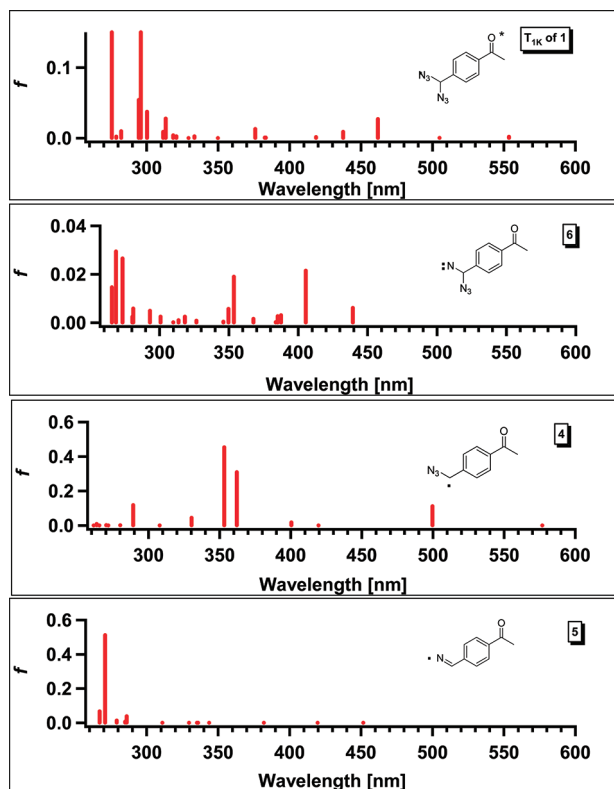


Figure 4. TD-DFT (B3LYP/6-31+G(d)) calculated UV spectrum of the T_{1K} of **1**, **6**, **4**, and **5** using TD-DFT level of theory with a 6-31+G(d) basis set.

nitrene **6**, indicating that a small amount of **6** was formed from the photolysis of **1** in competition with radical **4**.

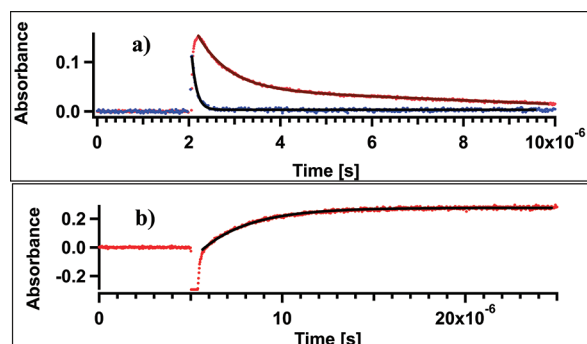


Figure 5. Kinetic trace obtained at (a) 480 nm in argon- (red trace) and oxygen-saturated (blue trace) acetonitrile and (b) 340 nm in argon-saturated acetonitrile.

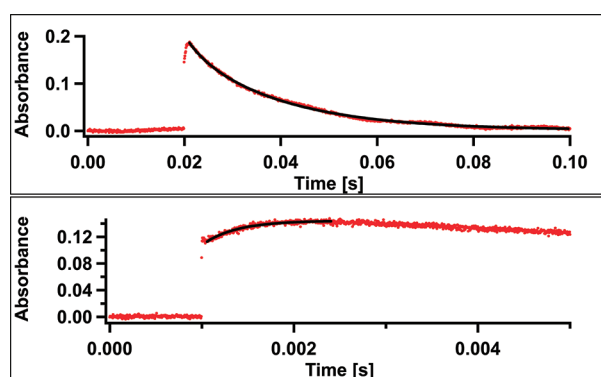


Figure 6. Kinetic traces obtained at 340 nm from laser flash photolysis of **1** in argon-saturated acetonitrile at different time scales.

In oxygen-saturated solution, the transient from **4** formed faster than the resolution of the laser (pulse width of 17 ns). Thus, by assuming that the concentration of oxygen in acetonitrile was 9.1×10^{-3} M, the T_{1K} of **1** must be quenched with oxygen with a rate constant of more than 6×10^9 s $^{-1}$ M $^{-1}$, which is comparable to what has been measured for acetophenone in acetonitrile (3.7×10^9 s $^{-1}$ M $^{-1}$)²⁴ and *p*-methyl acetophenone (see Supporting Information). In oxygen-saturated acetonitrile, the decay of **4** can be fitted as a monoexponential function to yield a rate constant of 1.2×10^7 s $^{-1}$, and the rate of oxygen quenching **4** in acetonitrile can be estimated to be approximately 1.3×10^9 M $^{-1}$ s $^{-1}$, which is similar to what has been reported for other carbon-based radicals.^{37–39}

Laser flash photolysis demonstrated that the major reactivity of **1** in solution is to form radical **4**, which expels a nitrogen molecule to form iminyl radical **5**. In oxygen-saturated solution, the triplet ketone becomes shorter lived than the time resolution of the laser, and radical **4** is formed in decreased yields. Furthermore, radical **4** is efficiently trapped with molecular oxygen. Because we observed a small growth at 340 nm, we theorize that a small amount of triplet nitrene **6** is formed and it slowly forms radical **5**.

2.5. Matrix Isolation. We investigated the photochemistry of **1** in argon matrices at 14 K to identify its reactivity in the absence of diffusion. We deposited **1** into argon matrices in several different experiments by placing a sample of **1** in a small stainless steel side arm, connected to the deposition line by an UltraTorr

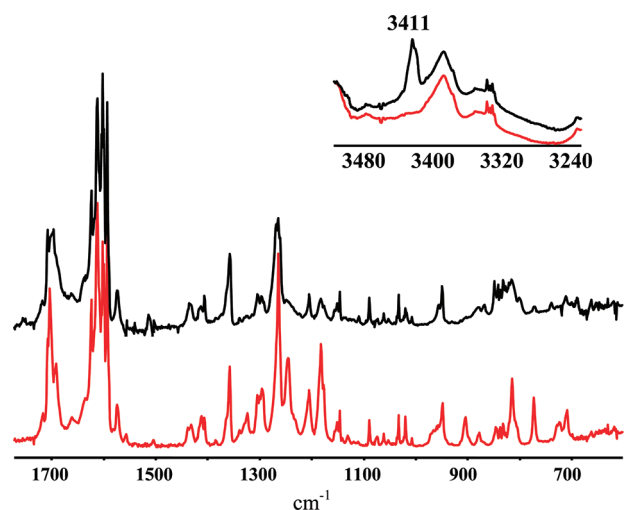


Figure 7. Photolysis of **1** in argon matrices (a) before irradiation (red) and (b) after irradiation (black).

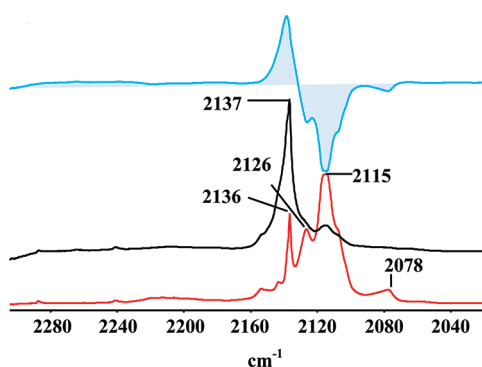


Figure 8. (a) Before irradiation (red) and (b) after irradiation (black) of **1**; (c) difference spectra (blue).

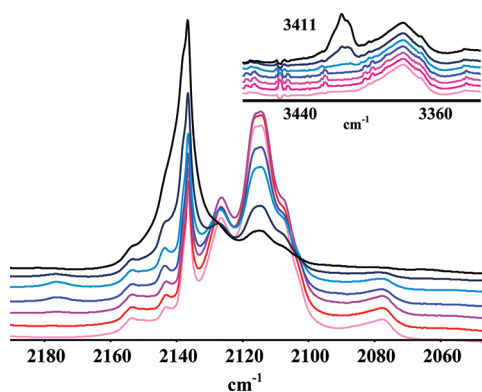


Figure 9. Irradiation of **1** as a function of time: (a) before irradiation (pink) and after (b) 1 min (red); (c) 11 min (purple); (d) 41 min (dark blue); (e) 1 h and 41 min (light blue); (f) 3 h and 41 min (gray); (g) 18 h and 41 min (black) of irradiation.

tee. The vapor of the compound was entrained in flowing argon, and carried to the cold window and deposited. Irradiation of **1** in argon matrices led to the growth of new absorption bands, mostly occurring near those of the parent azide (Figure 7). This result was expected because the acetophenone moiety was not

Scheme 13

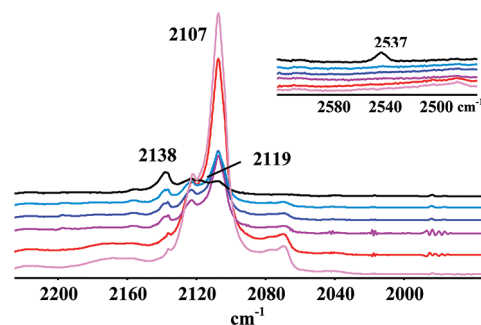
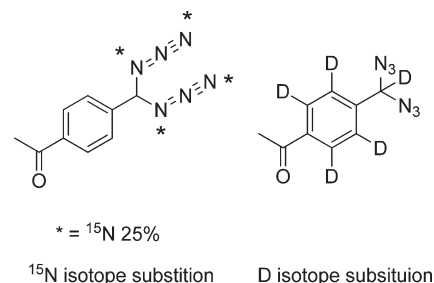


Figure 10. Photolysis of **1-d₅** as a function of time: (a) before the irradiation (pink) and after (b) 1 h (red); (c) 2.5 h (purple); (d) 3.5 h (dark blue); (e) 4.5 h (light blue); (f) 20 h (black) of irradiation.

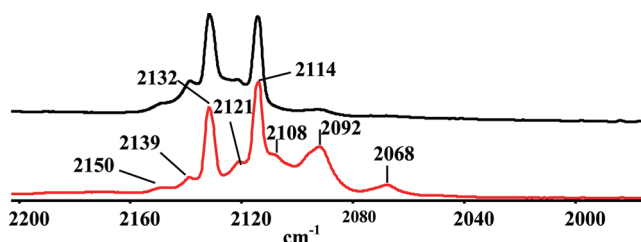


Figure 11. Photolysis of ¹⁵N isotope labeled **1** (a) before irradiation (red) and (b) after irradiation (black).

significantly affected by irradiation and the majority of the observed vibrational bands belonged to it. The infrared spectrum of **1** showed intense azido bands at 2136, 2126, 2115, and 2078 cm^{-1} (Figure 8 and Figure 9), which are all depleted upon irradiation. This multiplet of azido bands is likely due to different conformers of **1**, which additionally may be trapped in different matrix sites. After irradiation, a new azido band was observed at 2137 cm^{-1} . In addition, new bands were observed at 1269 and 850 cm^{-1} , which we assign to the formation of **6** on the basis of calculations.

To further verify that the azido band at 2137 cm^{-1} was due to the formation of **6**, we conducted similar experiments for deuterium- and ¹⁵N isotope-labeled **1** (**1-d₅** and **1-¹⁵N**, see Scheme 13). In **1-d₅**, five H atoms were fully replaced with deuterium atoms, whereas in **1-¹⁵N**, each azido moiety had either the α - or the γ -N atom as a ¹⁵N atom. Therefore, IR bands due to both ¹⁵N and ¹⁴N isotopes were observed. The infrared spectrum of **1-d₅** showed intense azido bands at 2122 and 2107 cm^{-1} and weaker ones at 2138 and 2069 cm^{-1} (Figure 10). The calculations

Table 1. Selected IR Bands Observed after Irradiation of **1** in Argon Matrices and Calculated IR Bands for **6**

	normal isotope		¹⁵ N		D × 5	
	obsd	calcd	obsd	calcd	obsd	calcd
N ₃	2137	2233 (442) ^a	2132	2231 (434) ^a	2138	2241 (320) ^a
			2114	2206 (442) ^a	2119	2217 (99) ^a
C–N	850	859 (30) ^a	850	859 (30) ^a	812	808 (9) ^a
				858 (30) ^a		
			842	853 (27) ^a		
				852 (27) ^a		

^a The values in parentheses are calculated oscillator strengths.

Table 2. Selected IR Bands after Prolonged Irradiation of **1** in Argon Matrices and Calculated IR Bands for **7**

stretch	normal isotope		¹⁵ N		D × 5	
	obsd	calcd	obsd	calcd	obsd	calcd
C=N–H	3411	3408 (5) ^a	3405	3408 (5) ^a	2537	2491 (5) ^a
				3400 (5) ^a		

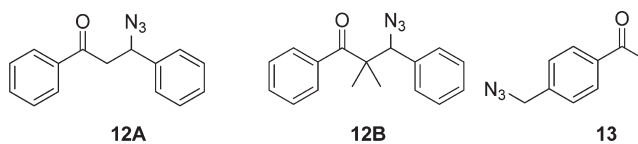
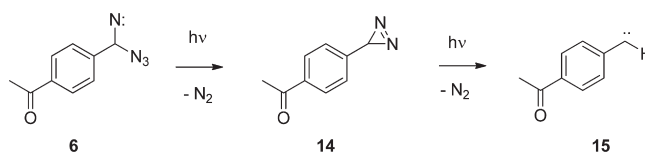
^a The values in parentheses are calculated oscillator strengths.

indicated that deuteration of **1** interchanges the symmetric and antisymmetric stretches of the two azido bands; therefore, the infrared spectrum of **1-d₅** was different from that for **1**. Upon irradiation, all azido bands were depleted beside the one at 2138 cm⁻¹, which grew in intensity, and a new band was formed at 2119 cm⁻¹. These results further supported the assignment of this band to **6**. The calculations showed that upon deuteration, the azido stretch in **6** coupled with the C–D stretch and the two azido vibrational bands had different intensities. Furthermore, the infrared spectrum of **1** formed from ¹⁵N-labeled sodium azide showed azido bands at 2150, 2139, 2132, 2121, 2114, 2108, 2092, and 2068 cm⁻¹ (Figure 11). After irradiation, the intensity of the azido bands at 2132 and 2114 cm⁻¹ increased, whereas the other azido bands were depleted. The azido bands that increased upon irradiation were placed 18 cm⁻¹ apart, which fits well with calculations showing how the ¹⁵N isotope labeling of **6** will shift the azido band 25 cm⁻¹.

An additional vibrational band identified at 850 cm⁻¹ was affected by ¹⁵N-isotope labeling and assigned to a C–N stretch in **6**, which was coupled to a stretching of the aromatic ring. Upon ¹⁵N-labeling, this band shifted to 842 cm⁻¹, which was in excellent agreement with the calculated shift of 6 cm⁻¹. This band shifted to 793 cm⁻¹ in **6-d₅** and its intensity also decreased and fit the calculations well (Table 1).

Prolonged irradiation of **1** in matrices resulted in a significant new band 3408 cm⁻¹, which was assigned to the N–H band in triplet **7**, based on its positions and calculations. The reactivity of **1** was monitored as a function of irradiation time to verify that **7** was formed by secondary photolysis of **6** (Figure 9 and Figure 10). Formation of the N–H band was observed after more than 4 h of irradiation, whereas the azido band due to the triplet nitrene **6** at 2137 cm⁻¹ was formed significantly faster.

Characterization of **7** was further supported by isotope labeling. For example, deuterium isotope labeling of **7** shifted the N–H band by 874 cm⁻¹, fitting well with the calculated shift of 917 cm⁻¹ (Table 2). We were not able to identify any additional vibrational bands for **7** that were affected by ¹⁵N isotope labeling,

Scheme 14**Scheme 15**

presumably because the intensity of the imine stretches are low, as further supported by the calculations.

3. DISCUSSION

We have shown that diazide **1** undergoes efficient azido cleavage in solution to form radical **4**, which expels a nitrogen molecule to form radical **5**. In addition to the azido cleavage, we theorized that **1** also forms a small amount of triplet alkyl nitrene **6**. We have shown previously that azide **12A**, **12B**, and **13** also undergo azido cleavage in competition with energy transfer to form triplet alkyl nitrene intermediates (Scheme 14).^{21,22} Radical stabilizing substituents adjacent to the azido moiety lower the transition state barrier for the azido cleavage, which explains why **1**, **12**, and **13** all undergo efficient azido cleavage in solution.

In comparison, photolysis of **1** in argon matrices does not lead to azido cleavage, but rather the formation of triplet alkyl nitrene intermediates. This result is similar to what we observed for azides **12A** and **12B** as well. It is possible that azides **1** and **12A** and **12B** undergo azido cleavage in matrices but the radical pair recombines because they cannot diffuse apart. However, it is also possible that the thermal population of the excited state that is the precursor to the azido cleavage is not feasible at low temperatures.

Prolonged irradiation of nitrene **6** does not lead to the formation of quintet dinitrene **8**, but rather triplet imine nitrene **7** via concurrent extrusion of a nitrogen molecule and an 1,2-H atom shift. The calculated transition state barrier for this reaction was 40 kcal/mol, and thus formation of **7** from **6** is feasible only photochemically. We propose that direct absorption by triplet **6** resulted in a triplet excited state of **6** and formation of **7**, and this process did not need the ketone moiety as a triplet sensitizer. Triplet sensitization of geminal diazo alkanes is not likely to yield quintet dinitrenes.

As mentioned above, Barash et al. studied triplet sensitized photolysis of 9,9-diazido-9H-fluorene with benzophenone, which resulted in the corresponding mononitrene; prolonged irradiation produced the triplet carbene (Scheme 2).¹⁶ It can be theorized that triplet nitrene **6** can react to form diazirine **14**, which upon irradiation forms triplet carbene **15**. We specifically looked for IR bands due to diazirine **14** and triplet carbene **15** in argon matrices, but we could not successfully identify formation of either compound. Nonetheless, we cannot rule out that small

amount of triplet carbene **15** was formed and that it is the precursor to products **3** and **11** (Scheme 15), especially since we do not eliminate oxygen in argon-saturated solutions but rather reduce the oxygen concentration.

4. CONCLUSION

It has been presented that photolysis of **1** in solution results in cleavage of one of the azido groups to form radical **4**, which expels a nitrogen molecule to form iminyl radical **5**. At cryogenic temperatures, **1** forms triplet alkyl nitrene **6**; however, prolonged irradiation of **6** does not yield dinitrene **8**, but rather triplet imine nitrene **7**.

5. EXPERIMENTAL SECTION

5.1. Calculations. All geometries were optimized at a B3LYP level of theory and with the 6-31+G(d) basis set as implemented in the Gaussian09 programs.^{25–27} All transition states were confirmed to have one imaginary vibrational frequency by analytical determination of the second derivatives of the energy with respect to internal coordinates. Intrinsic reaction coordinate calculations were used to verify that the located transition states corresponded to the attributed reactant and product.^{35,36} The absorption spectra were calculated using time-dependent density functional theory (TD-DFT).^{28–32} The effect of solvation was calculated using the self-consistent reaction field (SCRF) method with the integral equation formalism polarization continuum model (IEFPCM) with acetonitrile, methanol, and dichloromethane as solvents.^{40–44}

5.2. Laser Flash Photolysis. Laser flash photolysis was performed with an Excimer laser (308 nm, 17 ns).²³ The system has been described in detail elsewhere.²³ A stock solution of **1** in acetonitrile was prepared with spectroscopic grade acetonitrile, such that the solution had absorption between 0.3 and 0.6 at 308 nm. Typically, approximately 1 mL of the stock solution was placed in a 10 mm × 10 mm wide, 48 mm long quartz cuvette and was purged with argon for 5 min or oxygen for 15 min. The rates were obtained by fitting an average of two to five kinetic traces.

5.3. Matrix Isolations. Matrix isolation studies were performed using conventional equipment.⁴⁵

5.4. Preparation of 1. **5.4.1. Synthesis of 4-Dibromomethylacetophenone.** *p*-Methylacetophenone (1.8 g, 13 mmol) was dissolved in CCl₄ (30 mL), and *N*-bromosuccinimide (5.7 g, 32 mmol, 1:2.5 equiv) was added. A spatulum of benzoyl peroxide was added to the mixture, and the reaction was allowed to reflux while stirring for 20 h. The solvent was removed under vacuum, and the organic products were extracted with diethyl ether (50 mL). The extract was washed with water and dried over anhydrous MgSO₄. The solvent was removed under vacuum, and the crude *p*-dibromomethylacetophenone was crystallized in MeOH/acetone at 0 °C (2.4 g, 8.3 mmol, 33% yield). Mp: 66–68 °C. ¹H NMR (CDCl₃, 400 MHz): δ 2.6 (s, 3H), 6.7 (s, 1H), 7.7 (d, *J* = 8.4 Hz, 2H), 8.0 (d, *J* = 8.4 Hz, 2H) ppm. ¹³C NMR (CDCl₃, 100 MHz): δ 26.7, 39.6, 126.9, 128.7, 138.0, 146.1, 196.9 ppm. IR (CDCl₃): 3011, 1682 (s, C=O), 1605, 1575, 1505, 1409, 1357, 1263, 1228, 1185, 1146, 1114, 1073, 1014, 958, 835, 738, 698, 634, 611, 583 cm⁻¹. HRMS: *m/z* calculated for C₉H₉O⁷⁹Br₂ [M + H]⁺, 290.9020; found, 290.9016. GC/MS (EI): *m/z* 290 (M⁺), 275, 247, 210 (100%), 195, 183, 168, 141, 130, 115, 103, 89, 78.

5.4.2. Synthesis of 4-Diazidomethylacetophenone (1). 4-Dibromomethylacetophenone (2.4 g, 8.3 mmol) was dissolved in dry acetonitrile (15 mL). Azide exchange resin, (azide on Amberlite IRA-400, particle size 16–50 mesh, capacity 3.8 mmol/g, 8.8 g, 33.4 mmol, 1:4 equiv) was added to the mixture and allowed to stir for 21 days. The mixture was filtered, and the solvent was removed by air suction, yielding the crude

1-(4-diazidomethyl-phenyl)-ethanone (0.67 g, 3 mmol, 37% yield). ¹H NMR data was consistent with similar reported literature for analogous alkyl diazides.⁴⁶ ¹H NMR (CDCl₃, 400 MHz): δ 2.6 (s, 3H), 5.8 (s, 1H), 7.5 (d, *J* = 8 Hz, 2H), 8.0 (d, *J* = 8 Hz, 2H) ppm. ¹³C NMR (CDCl₃, 100 MHz): δ 26.7, 78.2, 126.7, 129.0, 138.1, 139.2, 197.3 ppm. IR (CDCl₃): 3060, 3006, 2926, 2106 (s, N₃), 1686 (s, C=O), 1610, 1576, 1508, 1412, 1360, 1339, 1304, 1290, 1266, 1247, 1185, 1116, 1075, 1017, 958, 898, 815, 767, 719, 637, 617, 596, 557 cm⁻¹. HRMS: *m/z* calculated for C₉H₈ON₆Na [M + Na]⁺, 239.0657; found, 239.0668.

5.4.3. Synthesis of Isotope Labeled 1. **5.4.3.1. Synthesis of 1-[4-(²H₃)Methyl(²H₄)phenyl]ethan-1-one (C₉D₇H₃O).** C₇D₈ (2.5 g, 25 mmol) was added to AlCl₃ (7.4 g, 55 mmol, 1:2.2 equiv)⁴⁷ in a round-bottom flask stored at 0 °C. Ac₂O (3.1 g, 30 mmol, 1:1.2 equiv) was dissolved in CH₂Cl₂ (30 mL) and added to the above mixture dropwise using a dropping funnel for 15 min while stirring. The reaction was allowed to proceed for 4.5 h. The reaction was chilled by pouring it into cold water (50 mL). One or two drops of HCl were added to the flask. The mixture was extracted using CH₂Cl₂ and water. The organic layer was dried using anhydrous MgSO₄ and was later filtered. The solvent was removed to obtain the crude product C₉D₇H₃O. (2.8 g, 19.6 mmol, 83% yield). ¹H NMR (CDCl₃, 400 MHz): δ 2.581 (s, 3H) ppm. ¹³C NMR (CDCl₃, 100 MHz): δ 20.3–21.1, 26.5, 127.8–128.4, 128.6–129.1, 134.6, 143.6, 197.8 ppm. IR (CDCl₃): 3004, 2255, 2120, 1682 (s, C=O), 1581, 1545, 1425, 1357, 1327, 1295, 1250, 1174, 1050, 1018, 950, 848, 824, 683, 640, 606, 548 cm⁻¹. HRMS: *m/z* calculated for C₉H₃²H₇ONa [M + Na]⁺, 164.10632; found, 164.10625.

5.4.3.2. Synthesis of 1-[4-[Dibromo(²H)methyl](²H₄)phenyl]ethan-1-one (C₉D₅H₃Br₂O). C₉D₇H₃O (1.5 g, 11 mmol) was dissolved in benzene (30 mL), and *N*-bromosuccinimide (4.8 g, 26 mmol, 1:2.2 equiv) was added. Two spatula of benzoyl peroxide were added to the reaction. The mixture was stirred for 20 h while refluxing. The solvent was removed, and the organic products were extracted using diethyl ether and water. The extract was dried using anhydrous MgSO₄, which was later filtered off. The solvent was removed to obtain the semioily crude C₉D₅H₃Br₂O. The crude product was purified using a silica column (10% ethyl acetate/90% *n*-hexane) (2.7 g, 9.1 mmol, 71% yield). ¹H NMR (CDCl₃, 400 MHz): δ 2.617 (s, 3H) ppm. ¹³C NMR (CDCl₃, 100 MHz): δ 26.615, 39.3–39.8, 126.2–126.7, 128.0–129.1, 136.7, 142.5, 197.3 ppm. IR (CDCl₃): 3065, 2928, 2203, 2139, 1786, 1715, 1683 (s, C=O), 1597, 1579, 1552, 1451, 1420, 1359, 1328, 1317, 1250, 1197, 1173, 1110, 1069, 1024, 953, 935, 851, 826, 778, 740, 712, 685, 656, 639, 627, 599, 551 cm⁻¹.

5.4.3.3. Synthesis of 1-[4-[Diazido(²H)methyl](²H₄)phenyl]ethan-1-one (C₉D₅H₃N₆O) (1-d₅). C₉D₅H₃Br₂O (0.4 g, 1.3 mmol) was dissolved in dry acetonitrile (25 mL), and azido exchange resin (azide on Amberlite IRA-400, particle size 16–50 mesh, capacity 3.8 mmol/g, 1.3 g, 5.1 mmol) reagent was added. The mixture was allowed to stir for 21 days. The mixture was filtered, and the supernatant was decanted. The solvent was removed to obtain the crude 1-d₅ (C₉D₅H₃N₆O, 0.14 g, 0.6 mmol, 50% yield). ¹H NMR (CDCl₃, 400 MHz): δ 2.622 (s, 3H) ppm. ¹³C NMR (CDCl₃, 100 MHz): δ 26.7, 77.5–78.0, 126.0–126.5, 128.1–128.5, 137.9, 139.0, 197.5 ppm. IR (CDCl₃): 3005, 2966, 2924, 2448, 2101 (s, N₃), 1686 (s, C=O), 1609, 1582, 1551, 1418, 1360, 1327, 1247, 1182, 1148, 1067, 1038, 1001, 954, 852, 825, 766, 692, 638, 620, 605, 557 cm⁻¹. HRMS: *m/z* calculated for C₉H₄²H₅ON₆ [M + H]⁺, 222.1152; found, 222.1150.

5.4.3.4. Synthesis of 1-[4-[(¹⁵N₂)Diazido]methyl]phenyl]ethan-1-one (C₉H₈¹⁵N₂N₄O) (1-¹⁵N). 4-Dibromomethylacetophenone (0.25 g, 0.86 mmol) was dissolved dry acetonitrile (40 mL). ¹⁵N-Na₃ (0.23 g, 3.4 mmol, 4 equiv) and azido exchange resin (azide on Amberlite IRA-400, particle size 16–50 mesh, capacity 3.8 mmol/g, 0.90 g, 3.4 mmol, 4 equiv) were added to the solution. The above mixture was allowed to stir for 21 days. The mixture was filtered, and the solvent was removed by air

suction to yield ^{15}N -substituted **1** (0.22 g, 0.8 mmol, 93% yield). ^1H NMR (CDCl_3 , 400 MHz): δ 2.63 (s, 3H), 5.80 (s, 1H), 7.54 (d, $J = 8$ Hz, 2H), 8.02 (d, $J = 8$ Hz, 2H) ppm. ^{13}C NMR (CDCl_3 , 100 MHz): δ 26.7, 78.1, 78.2, 126.7, 129.0, 138.1, 139.2, 197.3 ppm. ^{15}N NMR (CDCl_3 , 75 MHz), external standard ($\text{H}_2\text{NC}(\text{O})\text{NH}_2$): δ 93.1, 227.5, 262.1 ppm. IR (CDCl_3): 3281, 3060, 3006, 2923, 2345, 2087 (s, N_3), 1687 (s, $\text{C}=\text{O}$), 1610, 1577, 1508, 1412, 1359, 1338, 1304, 1290, 1266, 1239, 1179, 1115, 1075, 1017, 959, 895, 813, 764, 739, 712, 658, 637, 616, 596, 555, 500, 477 cm^{-1} . HRMS: m/z calculated for $\text{C}_9\text{H}_9\text{O}^{14}\text{N}_4^{15}\text{N}_2$ [$\text{M} + \text{H}$] $^+$, 219.0779; found, 219.0768.

5.5. Photolysis of 1. **5.5.1. Photolysis of 1 in Chloroform-*d* at 196 K.** A solution of **1** (~5 mg, 23 μmol) in CDCl_3 (1 mL) was purged with argon and photolyzed via a Pyrex filter for 4 h at 196 K. GC–MS analysis of the reaction mixture showed the formation of **2** and **3** in the ratio 4:1, with a small amount of remaining starting material. The products were characterized by GC–MS chromatography, ^1H NMR, ^{13}C NMR and IR spectroscopy of the reaction mixture. ^1H NMR and GC–MS data matched with reported literature.^{48,49} **2**: ^1H NMR (CDCl_3 , 400 MHz): δ 2.65 (s, 3H), 7.78 (d, $J = 8.4$ Hz, 2H), 8.05 (d, $J = 8.4$ Hz, 2H) ppm. ^{13}C NMR (CDCl_3 , 100 MHz): δ 26.8, 116.4, 118.0, 128.8, 132.5, 139.0, 196.5. IR (CDCl_3): 2231 (CN), 1687 ($\text{C}=\text{O}$) cm^{-1} . GC/MS (EI): m/z 145 (M), 130 (100%), 102, 75. **3**: ^1H NMR (CDCl_3 , 400 MHz): δ 2.671 (s, 3H), 7.988 (d, $J = 8.4$ Hz, 2H), 8.200 (d, $J = 8.4$ Hz, 2H), 10.117 (s, 1H) ppm. ^{13}C NMR (CDCl_3 , 100 MHz): δ 27.0, 128.7, 130.5, 139.9, 141.2, 191.6, 197.4 ppm. IR (CDCl_3): 1720 ($\text{C}=\text{O}$), 1687 ($\text{C}=\text{O}$) cm^{-1} . GC/MS (EI): m/z 148 (M), 133 (100%), 119, 105, 77.

5.5.2. Photolysis of 1 in Toluene. **5.5.2.1. Photolysis of 1 in Nitrogen-Saturated Toluene at 298 K.** A solution of **1** (~60 mg, 0.28 mmol) in Toluene (10 mL) was purged with nitrogen for 15 min and photolyzed via a Pyrex filter for 4 h at 298 K. GC–MS analysis of the reaction mixture showed the formation of **2** (40%), **3** (24%), **10** (30%), **11** (6%). In addition the GC–MS analysis showed formation of 1,2-diphenylethane from the solvent. **2**: GC/MS (EI): m/z 145 (M^+), 130 (100%), 102, 75. **3**: GC/MS (EI): m/z 148 (M^+), 133 (100%), 105, 77. **10**: GC/MS (EI): m/z 237 (M^+), 194, 104, 91 (100%), 76, 65. **11**: GC/MS (EI): m/z 224 (M^+), 209, 181, 133, 118, 105, 91 (100%), 77, 65. 1,2-Diphenylethane ($\text{C}_{14}\text{H}_{14}$): GC/MS (EI): m/z 182 (M^+), 165, 91 (100%), 65.

5.5.2.2. Photolysis of 1 in Oxygen-Saturated Toluene at 298 K. A solution of **1** (~60 mg, 0.28 mmol) in toluene (10 mL) was purged with oxygen for 15 min and photolyzed via a Pyrex filter for 4 h at 298 K. GC–MS analysis of the reaction mixture showed the formation of **2** (81%), **3** (7%) and **11** (12%). **2**: GC/MS (EI): m/z 145 (M), 130 (100%), 102, 75. **3**: GC/MS (EI): m/z 148 (M), 133 (100%), 105, 77. **11**: GC/MS (EI): m/z 224 (M), 209 (100%), 178, 165, 152, 105, 89, 77, 65.

■ ASSOCIATED CONTENT

Supporting Information. Cartesian coordinates, energies, and vibrational frequencies of **1–8** and NMR spectra of **1**, **1-*d*₅**, **1-¹⁵N**, **2**, and **3**. This material is available free of charge via the Internet at <http://pubs.acs.org>.

■ AUTHOR INFORMATION

Corresponding Author

*E-mail: anna.gudmundsdottir@uc.edu.

■ ACKNOWLEDGMENT

This work was supported by the National Science Foundation and the Ohio Supercomputer Center. R.A.A.U.R. is grateful for

support from the University Research Council at the University of Cincinnati and for a Harry B. Mark fellowship.

■ REFERENCES

- (1) Platz, M. S. In *Reactive Intermediate Chemistry*; Moss, R. A., Platz, M. S., Jones, M., Jr., Eds.; John Wiley & Sons, Inc.: New York, 2004; p 501.
- (2) Ling, C.; Minato, M.; Lahti, P. M.; Van, W. H. *J. Am. Chem. Soc.* **1992**, *114*, 9959.
- (3) Matsumoto, T.; Ishida, T.; Koga, N.; Iwamura, H. *J. Am. Chem. Soc.* **1992**, *114*, 9952.
- (4) Chapyshev, S. V.; Grote, D.; Finke, C.; Sander, W. *J. Org. Chem.* **2008**, *73*, 7045.
- (5) Chapyshev, S. V.; Misochko, E. Y.; Akimov, A. V.; Dorokhov, V. G.; Neuhaus, P.; Grote, D.; Sander, W. *J. Org. Chem.* **2009**, *74*, 7238.
- (6) Chapyshev, S. V.; Neuhaus, P.; Grote, D.; Sander, W. *J. Phys. Org. Chem.* **2010**, *23*, 340.
- (7) Kyba, E. P.; Abramovitch, R. A. *J. Am. Chem. Soc.* **1980**, *102*, 735.
- (8) *Decomposition of Organic Azides*; Abramovitch, R. A., Kyba, E. P., Eds.; John Wiley & Sons: London, 1971.
- (9) Singh, P. N. D.; Mandel, S. M.; Sankaranarayanan, J.; Muthukrishnan, S.; Chang, M.; Robinson, R. M.; Lahti, P. M.; Ault, B. S.; Gudmundsdottir, A. D. *J. Am. Chem. Soc.* **2007**, *129*, 16263.
- (10) Singh, P. N. D.; Mandel, S. M.; Robinson, R. M.; Zhu, Z.; Franz, R.; Ault, B. S.; Gudmundsdottir, A. D. *J. Org. Chem.* **2003**, *68*, 7951.
- (11) Klima, R. F.; Gudmundsdottir, A. D. *J. Photochem. Photobiol., A* **2004**, *162*, 239.
- (12) Sankaranarayanan, J.; Bort, L. N.; Mandel, S. M.; Chen, P.; Krause, J. A.; Brooks, E. E.; Tsang, P.; Gudmundsdottir, A. D. *Org. Lett.* **2008**, *10*, 937.
- (13) Mandel, S. M.; Bauer, J. A. K.; Gudmundsdottir, A. D. *Org. Lett.* **2001**, *3*, 523.
- (14) Moriarty, K. M.; Kliegman, J. M.; Shovlin, C. *J. Am. Chem. Soc.* **1967**, *89*, 5958.
- (15) Moriarty, R. M.; Kliegman, J. M. *J. Am. Chem. Soc.* **1967**, *89*, 5959.
- (16) Barash, L.; Wasserman, E.; Yager, W. A. *J. Am. Chem. Soc.* **1967**, *89*, 3931.
- (17) *Azides and Nitrenes: Reactivity and Utility*; Scriven, E. F. V., Ed.; Academic Press: New York, 1984.
- (18) Muthukrishnan, S.; Mandel, S. M.; Hackett, J. C.; Singh, P. N. D.; Hadad, C. M.; Krause, J. A.; Gudmundsdottir, A. D. *J. Org. Chem.* **2007**, *72*, 2757.
- (19) Wagner, P. J.; Kempainen, A. E. *J. Am. Chem. Soc.* **1968**, *90*, 5898.
- (20) Wagner, P.; Park, B. S. *Org. Photochem.* **1991**, *11*, 227.
- (21) Klima, R. F.; Jadhav, A. V.; Singh, P. N. D.; Chang, M.; Vanos, C.; Sankaranarayanan, J.; Vu, M.; Ibrahim, N.; Ross, E.; McCloskey, S.; Murthy, R. S.; Krause, J. A.; Ault, B. S.; Gudmundsdottir, A. D. *J. Org. Chem.* **2007**, *72*, 6372.
- (22) Ranaweera, R. A. A. U.; Zhao, Y.; Muthukrishnan, S.; Keller, C.; Gudmundsdottir, A. D. *Aust. J. Chem.* **2010**, *63*, 1645.
- (23) Muthukrishnan, S.; Sankaranarayanan, J.; Klima, R. F.; Pace, T. C. S.; Bohne, C.; Gudmundsdottir, A. D. *Org. Lett.* **2009**, *11*, 2345.
- (24) Murov, S. L.; Carmichael, I.; Hug, G., L. *Handbook of Photochemistry*, 2nd ed.; Marcel Dekker, Inc.: New York, 1993.
- (25) Frisch, M. J. T.; G. W.; Schlegel, H. B.; Scuseria, G. E.; Robb, M. A.; Cheeseman, J. R.; Montgomery, Jr., J. A.; Vreven, T.; Kudin, K. N.; Burant, J. C.; Millam, J. M.; Iyengar, S. S.; Tomasi, J.; Barone, V.; Mennucci, B.; Cossi, M.; Scalmani, G.; Rega, N.; Petersson, G. A.; Nakatsuji, H.; Hada, M.; Ehara, M.; Toyota, K.; Fukuda, R.; Hasegawa, J.; Ishida, M.; Nakajima, T.; Honda, Y.; Kitao, O.; Nakai, H.; Klene, M.; Li, X.; Knox, J. E.; Hratchian, H. P.; Cross, J. B.; Bakken, V.; Adamo, C.; Jaramillo, J.; Gomperts, R.; Stratmann, R. E.; Yazyev, O.; Austin, A. J.; Cammi, R.; Pomelli, C.; Ochterski, J. W.; Ayala, P. Y.; Morokuma, K.; Voth, G. A.; Salvador, P.; Dannenberg, J. J.; Zakrzewski, V. G.; Dapprich, S.; Daniels, A. D.; Strain, M. C.; Farkas, O.; Malick, D. K.; Rabuck, A. D.; Raghavachari, K.; Foresman, J. B.; Ortiz, J. V.; Cui, Q.; Baboul, A. G.; Clifford, S.; Cioslowski, J.; Stefanov, B. B.; Liu, G.; Liashenko, A.

Piskorz, P.; Komaromi, I.; Martin, R. L.; Fox, D. J.; Keith, T.; Al-Laham, M. A.; Peng, C. Y.; Nanayakkara, A.; Challacombe, M.; Gill, P. M. W.; Johnson, B.; Chen, W.; Wong, M. W.; Gonzalez, C.; Pople, J. A. *Gaussian09*; Gaussian Inc.: Wallingford, CT, 2003.

- (26) Becke, A. D. *J. Chem. Phys.* **1993**, *98*, 5648.
- (27) Lee, C.; Yang, W.; Parr, R. G. *Phys. Rev. B: Condens. Matter* **1988**, *37*, 785.
- (28) Stratmann, R. E.; Scuseria, G. E.; Frisch, M. J. *J. Chem. Phys.* **1998**, *109*, 8218.
- (29) Parr, R. G.; Weitao, Y. *Density Functional Theory in Atoms and Molecules*; Oxford University Press: Oxford, 1989.
- (30) *Density Functional Methods in Chemistry*; Labanowski, J. K., Andzelm, J. W., Eds.; Springer-Verlag: New York, 1991.
- (31) Foresman, J. B.; Head-Gordon, M.; Pople, J. A.; Frisch, M. J. *J. Phys. Chem.* **1992**, *96*, 135.
- (32) Bauernschmitt, R.; Ahlrichs, R. *Chem. Phys. Lett.* **1996**, *256*, 454.
- (33) Muthukrishnan, S.; Sankaranarayanan, J.; Pace, T. C. S.; Konosonoks, A.; De Michiei, M. E.; Meese, M. J.; Bohne, C.; Gudmundsdottir, A. D. *J. Org. Chem.* **2010**, *75*, 1393.
- (34) Nguyen, M. T.; Sengupta, D.; Ha, T.-K. *J. Phys. Chem.* **1996**, *100*, 6499.
- (35) Gonzalez, C.; Schlegel, H. B. *J. Chem. Phys.* **1989**, *90*, 2154.
- (36) Gonzalez, C.; Schlegel, H. B. *J. Phys. Chem.* **1990**, *94*, 5523.
- (37) Font-Sanchis, E.; Aliaga, C.; Bejan, E. V.; Cornejo, R.; Scaiano, J. C. *J. Org. Chem.* **2003**, *68*, 3199.
- (38) Frenette, M.; MacLean, P. D.; Barclay, L. R. C.; Scaiano, J. C. *J. Am. Chem. Soc.* **2006**, *128*, 16432.
- (39) Korth, H.-G. *Angew. Chem., Int. Ed.* **2007**, *46*, 5274.
- (40) Tomasi, J.; Mennucci, B.; Cammi, R. *Chem. Rev.* **2005**, *105*, 2999.
- (41) Mennucci, B.; Cancès, E.; Tomasi, J. *J. Phys. Chem. B* **1997**, *101*, 10506.
- (42) Cancès, E.; Mennucci, B. *J. Chem. Phys.* **2001**, *114*, 4744.
- (43) Tomasi, J.; Persico, M. *Chem. Rev. (Washington, DC)* **1994**, *94*, 2027.
- (44) Cramer, C. J.; Truhlar, D. G. *Chem. Rev. (Washington, DC)* **1999**, *99*, 2161.
- (45) Ault, B. S. *J. Am. Chem. Soc.* **1978**, *100*, 2426.
- (46) Nishiyama, K.; Oba, M.; Watanabe, A. *Tetrahedron* **1987**, *43*, 693.
- (47) Noller, C. R.; Adams, R. *J. Am. Chem. Soc.* **1924**, *46*, 1889.
- (48) Chen, G.; Weng, J.; Zheng, Z.; Zhu, X.; Cai, Y.; Cai, J.; Wan, Y. *Eur. J. Org. Chem.* **2008**, 3524.
- (49) Liu, S.; Berry, N.; Thomson, N.; Pettman, A.; Hyder, Z.; Mo, J.; Xiao, J. *J. Org. Chem.* **2006**, *71*, 7467.